Accepted Manuscript

Characterisation of the intracellular protozoan MPX in Scottish mussels, *Mytilus edulis* Linnaeus, 1758

G. Fichi, S. Carboni, J.E. Bron, J. Ireland, M.J. Leaver, G. Paladini

Characterisation of the intracellular protozoan MPX in Scottish mussels, *Mytilus edulis* Linnaeus, 1758

G. Fichi *[a], S. Carboni [a], J.E. Bron [a], J. Ireland [a], M.J. Leaver [a], G. Paladini [a]

[a] *Institute of Aquaculture, Faculty of Natural Sciences, University of Stirling, FK9 4LA, Stirling, UK*

Running title: Characterisation of MPX

Key words: mussel protozoan X, Rhynchodida, ciliate, bivalve, digestive gland, phylogeny

*Corresponding author: Gianluca Fichi, Institute of Aquaculture, Faculty of Natural Sciences, University of Stirling, FK9 4LA, Stirling, UK. Email: gianluca.fichi@gmail.com

1

Abstract:

Ciliates have been reported as pathogens of many species of economically important bivalves. Mussel protozoan X (MPX), is an uncharacterised intracellular ciliate of mussels and has been widely reported in *Mytilus spp*. around the world. In order to characterise this ciliate, *Mytilus edulis* samples were collected from a site on the West coast of Scotland, and four different fixatives for histological examination were tested. Fresh preparations of mussel digestive glands were also examined by laser scanning confocal microscopy. Intracellular ciliates were prepared by laser capture microdissection and partial sequences of small subunit ribosomal RNA gene and of large subunit ribosomal RNA gene were generated, using Phyllopharyngea primers. Methacarn solution proved to be the best fixative for both histological and molecular characterisation. The morphological and molecular investigations confirmed that this ciliate belongs to the class Phyllopharyngea, order Rhynchodida. However, this organism does not belong to any known family, genus or species, therefore, a new description is necessary, following further morphological analyses. Most mussel samples containing MPX displayed mild to moderate infections, with no signs of necrosis or haemocytic response, although a single sample displayed a severe infection ($\sim10^3$ ciliates per section). The localisation of this ciliate in tissues other than the digestive gland, the presence of necrosis in infected tissue of the most severely infected mussel and the binary fission of this ciliate have been observed here for the first time. We also report the first observation of the live ciliate isolated from tissue. Although MPX remains of unknown significance to the mussel industry, tools and protocols described here will be useful in further characterising these and other ciliates (subclass Rhynchodia) known as pathogens for bivalves.

1. **Introduction**

Ciliates, ubiquitous protozoans belonging to the phylum Ciliophora, have been reported in many species of economically important bivalves, including mussels (Zeidan et al., 2012). Some of them are extracellular, and live as commensals in the lumen of the digestive gland tubules and acini, such as *Stegotricha enterikos* Bower and Meyer, 1993 (Bower and Meyer, 1993) or *Ancicostroma* sp. (Cova et al., 2015), or in association with or attached to the gills, such as *Trichodina* spp. (Xu et al., 2000). However, some can also invade the extrapallial space and coelomic cavity, for example orchitophryid ciliates (Elston et al., 1999). Others are intracellular and parasitise gills, such as *Sphenophrya* sp., which causes xenomas (McGurk et al., 2016), or live in digestive tubule epithelia without signs of haemocytic response, such as the uncharacterised "mussel protozoan X" (MPX), (Gombac et al., 2008; Spiers, 2008; Villalba et al., 1997), which is the subject of this study.

MPX is a common and widespread associate of mussels and has also been reported as a "Ciliophora-like organism" (CILO) (Robledo et al., 1994), "Rhynchodida-like ciliate" (Gombac et al., 2008), "intracellular ciliate of mussels" or "digestive gland ciliate" (Bower, 2013). MPX is found in digestive tubule epithelia of *Mytilus edulis* Linnaeus, 1758, *Mytilus trossulus* Gould, 1850 and *Mytilus galloprovincialis* Lamarck, 1819, and is suggested to belong to the class Phyllopharyngea (see Bower, 2013).

Following the classification reported by Lynn (2008), the class Phyllopharyngea comprises four subclasses: Cyrtophoria, Chonotrichia, Rhynchodia and Suctoria (Lynn, 2008). Rhynchodians are found particularly in gills of mollusca and other invertebrates (Lynn, 2008). MPX has previously been reported as a Rhynchodida-like ciliate (Gombac et al., 2008), this being one of the two orders of the Rhynchodia subclass. The members of the subclass Rhynchodia are characterised by a single suctorial tube lined with microtubular phyllae, called a "tentacle" and visible as a protuberance located at the anterior end of the

ciliate, while the two orders, Hypocomatida Deroux, 1976 and Rhynchodida Chatton *et Lwoff*, 1939, can be discriminated by the distribution of kineties (rows of flagella / cilia), (Lynn, 2008). Some hypocomatids are predators of suctorians and peritrichs, while others are parasites of ascidians and barnacles (Lynn, 2008). On the other hand, rhynchodids are considered obligate parasites of bivalves (Lynn, 2008). However, they have also been reported in other molluscs and invertebrates with a narrow host preference, although adjacent hosts can also be infected (Lynn, 2008). The intensity of infection of these ciliates rarely reaches levels that cause damage to their hosts (Lynn, 2008).

MPX has been described as a drop, pear, or spindle-shaped organism, covered with nine oblique rows of cilia encircling the cell, and a longest axis length varying between 3.9-16 µm, while the smallest axis length varies between 2.3-8.4 µm (Robledo et al., 2014; Gombac et al., 2008; Spiers, 2008; Villalba et al., 1997; Figueras et al., 1991). In histological sections, the nuclear apparatus has been described as being polymorphic, oval to globular, multi-lobed or fragmented into several nuclei of varying size, sometimes condensed into a macronucleus (Robledo et al., 2014; Gombac et al., 2008; Spiers, 2008; Villalba et al., 1997; Figueras et al., 1991). A densely staining rod, similar to a cytopharyngeal structure, has been noted by some authors (Spiers, 2008).

In several studies, MPX has been observed in the digestive cells of the secondary digestive tubules of mussels, but not in pyramidal basophilic cells (Robledo et al., 1994; Figueras et al., 1991), and, in particular, it has been reported within the apical portion of the cytoplasm of the digestive tubule epithelia, inside vacuoles (Spiers, 2008; Villalba et al., 1997). More than one MPX has often been found in a single infected tubule and, more rarely, up to two MPXs have been observed in the same host cell (Gombac et al., 2008; Spiers, 2008; Villalba et al., 1997). In moderate infections, MPX has also been observed in the lumen of digestive tubules (Gombac et al., 2008).

4

Despite the ability of these ciliates to disrupt the cells of the digestive tubules during heavy infections, (Bower, 2013), no signs of haemocytic response, mortality or growth reduction have been reported in mussels (Robledo et al., 2014; Bower, 2013; Gombac et al., 2008; Spiers, 2008; Villalba et al., 1997; Figueras et al., 1991). However, during 2001-2002, an infection with a Rhynchodid-like ciliate, similar to MPX, was reported in the digestive tubules of silverlip pearl oysters, *Pinctada maxima* (Jameson, 1901) in Western Australia (Spiers, 2008; Spiers et al., 2008). In the outbreak reported in the silverlip pearl oysters, the presence of the intracellular ciliate was significantly correlated to the severity of the host's haemocytic response (Spiers, 2008; Spiers et al., 2008). Affecting only silverlip pearl oysters under 70 mm, the outbreak was not considered to be a major risk to the pearl industry, however, it was supposed that the parasite was associated with the mortality of the smaller oysters (Spiers, 2008).

In mussels, MPX has been observed in several European countries and in Canada (Broughton, 2016; Bower, 2013; Carella and De Vico, 2012; Bignell et al., 2011; Villalba et al., 1997; Figueras et al., 1991) with an observed prevalence of less than 1% (Gombac et al., 2008) up to 100% (Bower, 1992). Although MPX has been widely reported, its characterisation is still uncertain. The aim of the present study was to better morphologically and molecularly characterise this ciliate in *Mytilus edulis* in Scotland. The development of diagnostic protocols for the characterisation of MPX could provide a useful contribution to the investigation of this and other members of the Phyllopharyngea, some of which are considered obligate parasites of bivalves, and others intracellular organisms in shellfish.

2. Materials and methods

2.1 Samples

5

From April to June 2017, five separate samplings of 10 mussels each were collected from the West coast of Scotland from a population of wild mussels previously known as MPX positive (N 56° 29′ 41.8534″, W 5° 27′ 23.3744″). The samples were stored at 4°C until processed. Within 24 h from collection, the shell of each animal was measured and a single identification number was given to each shellfish. Digestive diverticula were collected and half of the digestive gland was individually fixed in 10% buffered formalin, used as a reference fixative, and the other half was randomly fixed in PAXgene Tissue FIX Container (Pg) (Qiagen, Germany), 95% ethanol (95% EtOH), or Methacarn (MthC) solution (Puchtler et al., 1970), for histological examination. In addition, a small amount of digestive gland of each sample was fixed in 95% EtOH, and in MthC for molecular examination. Small sections of the digestive gland of some individuals were also collected for fresh examination to in order to recover live ciliates.

2.2 Histological examination

Formalin fixed samples were processed according to standard procedures. In order to avoid formalin contamination, Pg fixed samples were manually processed as reported in the PreAnalytiX supplementary protocol following the manufacturer's instruction, while MthC fixed samples and 95% EtOH fixed samples were processed using the following protocol: absolute ethanol for 1 h and 30 min (3 changes), Xylene for 1 h (2 changes), and Paraffin (60°C) for 2 h (2 changes). After the paraffin embedding, 5 µm sections were stained with haematoxylin and eosin (H&E) and examined using an Olympus BX53 microscope. The severity of the infection was evaluated when samples proved positive at 20× magnification, and was classified as follows, based on the number of ciliates per slide in a histological section: mild (less than 20 ciliates), moderate (20-50) and severe (more than 50), as described by Gombac *et al.* (2008).

2.3 Laser scanning confocal microscopy

From MPX positive formalin fixed samples, slices of 5 µm were cut and stained with eosin and 4',6-Diamidino-2-Phenylindole (DAPI) (Molecular Probes, Invitrogen) for nuclear staining. In summary, some drops of 300 nM solution of DAPI dissolved in deionised water were added to the slides after eosin staining and kept in the dark for 15 min. After that, the excess DAPI stain was removed through a water wash, and the slides were dehydrated following standard procedures for histological sections. A Leica SP2 AOBS confocal scanning laser microscope (CSLM) and a DM TRE2 inverted microscope (Leica Microsystems) were used to observe the prepared slides.

2.4 Fresh examination

A small section of digestive gland was compressed between the slide and the coverslip with a drop of filtered sea water and examined using Differential Interference Contrast (DIC) fitted to an Olympus BX53 microscope in order to find the MPX in the tissue.

2.5 Laser capture microdissection

In order to collect MPX for molecular analyses, laser capture microdissection was performed. To evidence MPX in the digestive tubule cells, 3 µm sections were cut from paraffin embedded blocks, dehydrated, and stained with H&E or with 0.01% ethidium bromide for 3 min. The collection of MPX was applied after 20 µm infra-red (IR) laser cutting using Arcturus® CapSure macro LCM caps (Applied Biosystems, USA) with an Arcturus® Laser Capture Microdissection system (Thermo Fisher Scientific) in bright light for H&E stained slides and triple filter fluorescent light (Triple Dichroic filter, DAPI/FITC/TRITC, Excitation (nm) = 385-400/475-493/545-565, Emission (nm) = 450-

7

465/503-533/582-622) for 0.01% ethidium bromide stained slides. In order to obtain a sufficient number of MPX per cap, only the samples that were scored as severely infected were used.

2.6 DNA extraction

DNA was extracted from 25 mg of 95% EtOH or MthC fixed digestive glands using DNA Blood & Tissue kit (Qiagen, Germany). DNA from MPX collected with the laser capture microscope was extracted using Arcturus® PicoPure DNA extraction kit (Applied Biosystems, USA) following the manufacturer's instructions.

2.7 Phyllopharyngea primers design, PCR, and sequencing

Gene sequences for α-tubulin, small subunit ribosomal RNA (SSU) and large subunit ribosomal (LSU) RNA of Phyllopharyngea were retrieved from the GenBank database and aligned using Bioedit software (Hall, 1999). Based on the alignment, conserved regions in Phyllopharyngea for each gene were chosen and sets of primers were designed. Primers were tested *in silico* for specificity to Phyllopharyngea, whilst excluding Mollusca using Primer Blast against the GenBank nr-database. This resulted in the primers reported in Table 1. Gradient PCR was carried out on DNA of histologically positive samples with each primer pair to determine the optimum annealing temperature and to ensure specific amplifications using MyTaq™ mix (Bioline, UK). The following PCR protocols were applied: an initial denaturing step at 95 °C for 1 min, followed by 38 cycles of denaturation at 95 °C for 15 s, annealing for 15 s at 60 °C for α-tubulin, 68.5 °C for LSU, and 61 °C for SSU amplification, denaturation at 72 °C for 30 s, and a final step of 72 °C for 7 min as elongation. For each set of primers, DNA from three histologically positive samples (low, mild, and severe MPX infection) and three histologically negative samples

8

were tested. PCR products were purified through QIAquick PCR Purification kit (Qiagen, Germany), or with QIAquick Gel Extraction kit (Qiagen, Germany) when the PCR produced more than one segment of amplification, and sequencing was outsourced to GATC Biotech.

2.8 Phylogenetic analysis

The sequences obtained were compared with GenBank sequences using nucleotide BLAST. The phylogenetic analysis was conducted including the sequences of Phyllopharyngea species deposited in GenBank and, whenever possible, the sequences of the species that showed the highest similarity with the obtained sequencing products in BLAST for each family of Ciliophora reported by Gao *et al.* (2016). The phylogenetic tree was generated using maximum-likelihood probability with a PhyML mode through Seaview software with 1000 bootstrap replicates (Gouy et al., 2010).

2.9 MPX primer design, PCR, and sequencing

In order to develop a more specific and sensitive PCR for MPX, sets of internal primers were designed on SSU sequence, obtained as described above, using Primer Blast. The following set of internal primers, amplifying a 405 bp segment, was chosen after checking on Primer Blast to avoid non-specific amplifications: SSU MPX F 5'-ATA CGA ATG CCC CCA ACT GT-3' and R 5'-AGG AGC CTG AGA AAC GGC TA-3'.

PCR was performed using MyTaq™ mix (Bioline, UK) with the following thermal protocol: denaturation step of 95 °C for 1 min, followed by 35 cycles of 95 °C for 15 s, 65.5 °C for 15 s and 72 °C for 30 s, followed by a final step of 72 °C for 7 min. To be sure to have amplified MPX DNA and to exclude the amplification of other ciliates, this PCR was applied on DNA extracted from MPX collected through laser dissection capture. The

9

products were then sequenced and aligned with SSU sequence obtained as previously described. In addition, 15 histologically positive samples and 15 histologically negative samples, fixed in 95% EtOH and MthC solution, were tested with MPX PCR.

3. Results

3.1 Samples

The length and maximum width of *Mytilus edulis* were 5.55 cm (± 1.06 cm) and 2.71 cm (± 0.68 cm), respectively.

3.2 Histological examination

Fifteen samples out of 50 were observed to be infected with MPX, showing a prevalence of 30% (C.I. 95%, 17.30-42.70). The severity of infection was low (less than 20 ciliates per slide) in 12 out of 15 positive samples (80%), mild in one sample (21 ciliates per slide) (7%) and severe in two samples (51 ciliates per slide in one sample and more than 10^3 in the other) (13%).

No haemocytic response was observed around the infected digestive tubules. In the sample with more than 10^3 ciliates per slide, the disruption of some digestive tubule cells was observed (Fig. 1 a) with free ciliates in the lumen. This digestive gland was obtained from a mussel of 6.5 cm in length and 3.6 cm in width. No gross lesions were observed during the sampling. At histological examination, no signs of colliquative necrosis or epithelial atrophy were observed in the digestive tubules of this sample, but an enlargement of the digestive cells and the presence of lipofuscin granules were observed (Fig. 1 a). In the same sample, ciliates were found in the connective tissue around the digestive tubules that sometimes appeared necrotic (Fig. 1 b), but no signs of phagocytosis and/or encapsulation of the ciliates were observed, despite the fact that some haemocytes were noticed. Free

10

ciliates were also found in the stomach lumen (Fig. 1 c) and in the ovarian tissue, with tissues appearing necrotic but lacking evident signs of haemocytic response (Fig. 1 d).

In the most intensively infected sample, up to 50 ciliates per digestive tubule were observed, but not every tubule appeared infected and up to two MPXs per cell were found (Fig. 2). The length and the maximum width of the ciliates were 11.31 ($\pm$ 1.70) μm (range 9.19 − 19.78 μm) and 7.81 ($\pm$ 1.14) μm (range: 5.85 − 9.94 μm), respectively, and they appeared pear-shaped. Different stages of the ciliate were found, most of them showed several nuclei (Figs. 1-2), sometimes condensed in a big macronucleus (Figs. 3 a-b) with or without one evident micronucleus (Figs. 3 b-c). Multi-lobate nuclei were rarely observed (Fig. 2). Up to 14 round nuclei of several dimensions were counted, and in some ciliate a less strongly stained circular organelle was observed in the centre of them (Figs. 3 d). Some ciliates were found to be undergoing division inside the intracellular vacuoles (Figs. 3b). The division appeared as a transverse isotonic binary fission with the macronucleus in division and an accumulation of chromatin at the two poles followed by cytokinesis. Sometimes, the two micronuclei were evident as slightly stained objects at the two poles (Fig. 3b). In some ciliates, a structure similar to a cytopharynx was observed (Figs. 3 a).

An assessment of the different fixatives tested suggests that formalin fixed samples showed the best performance, with good conservation of the integrity of the tissue and an evident staining of the ciliates, followed by MthC solution and then by 95% EtOH fixed samples. In Pg fixed samples, nuclei of the ciliate were not very well stained in comparison to the cytoplasm and the ciliate was thus difficult to localise at 20× magnification. In all fixatives, the cilia were visible in some ciliates stained with H&E at 100x magnification using an Olympus BX53 microscope.

3.3 Laser scanning confocal microscopy

DAPI staining highlighted several nuclear patterns under confocal laser microscopy examination. Most ciliates appeared with several round nuclei without a clear connection between them (Fig. 4 a). Some ciliates showed a larger macronucleus with or without several smaller nuclei (Figs. 4 a-c), and sometimes the macronucleus was observed to be undergoing division (Fig. 4 b). In some ciliates, very small DAPI stained corpuscles were found at one or both poles of the macronucleus (Fig. 4 c). At the centre of the small nuclei, a non-DAPI stained round corpuscle was observed (Figs. 4 d-f). No multi-lobed or fragmented macronuclei were observed. No consistent pattern or grouping of subset dimensions of nuclei was evidenced and a maximum of 18 small nuclei were observed in any single ciliate.

3.4 Fresh examination

Ciliates were observed live, showing a slow, circular motion, moving inside the digestive gland tissue, but some ciliates were found free swimming on the slide, outside the tissue (Fig. 5 a). The body was observed to be banana-shaped, the length and the maximum width were respectively 20.50 (± 2.97) µm (range 15.67 – 21.62 µm) and 5.89 (± 2.27) µm (range: 2.00 – 7.80 µm), respectively, with cilia 8-9 µm long. Cytoplasm appeared colourless or greyish and several small round organelles were observed.

3.5 Laser capture microdissection

Ethidium bromide staining was demonstrated to be the most efficacious method to identify MPX, since the nuclei can be clearly highlighted (Fig. 5 b), allowing collection of more than 1,000 MPX per slide compared with around 400 MPX through H&E stained slides. No difference was noticed between formalin, 95% EtOH and MthC fixed samples in the

collection of MPX. No Pg fixed samples were severely infected and, therefore, these samples were not used in the laser dissection capture procedure.

3.6 Phyllopharyngea PCR and sequencing

Two histologically positive samples (severe and low MPX infected) and one histologically negative sample resulted in amplification of 742 bp of the α-tubulin gene showing a 93.82% identity to *Mytilus galloprovincialis* α-tubulin mRNA after a BLAST analysis. LSU gene amplification, resulted in amplicons of the predicted size only in the severely infected sample. After sequencing of this amplified fragment (449 bp, GeneBank ac. no. MF944083), BLAST analysis showed 86.45 % identity with the uncultured ciliate clone 10003B06 (GenBank ac. no. GU199592.1), and 66.67 % identity to *Mytilus* spp. SSU PCR amplified a ~ 900 bp segment in all samples tested and an additional segment of ~ 700 bp only in the severely infected sample. The sequencing of the 900 bp fragment failed to produce a sequence, indicating possible artefactual single primer amplification. However, the ~ 700 bp (653 bp after sequencing, GenBank ac. no. MF944084) amplicon from heavily infected samples showed 85.69 % identity with an uncultured phyllopharyngid, clone BS17_E5 (GenBank ac. no. FN598372.1), and only 13.63% identity to *Mytilus* spp.

3.7 Phylogenetic analysis

Through phylogenetic analysis, the LSU sequence clustered with the Phyllopharyngea species with the closest relationship being to *Hypocoma acetinarum* (GenBank acc. no. KM222157) with moderate support (89% ML) (Fig. 6). The phylogenetic analysis of SSU showed similar results. The SSU sequence clustered with the Phyllopharyngea species and, also in this case, was closest (64% ML) to *Hypocoma acetinarum* (GenBank acc. no. JN867019) (Fig. 7).

3.8 MPX PCR and sequencing

Using the MPX specific primers, the laser capture extracted DNA tested positive both in 95% EtOH and in MthC fixed slides, and both in H&E and in ethidium bromide staining slides. No amplification was obtained from formalin fixed slides. The sequencing of the 405 bp PCR products showed a 100% homology with the SSU sequence obtained from the severely infected sample. All histologically positive samples, and five out of 15 histologically negative samples tested positive with MPX amplification. No difference was observed between 95% EtOH and MthC fixed samples.

4. Discussion

MPX has been previously reported in UK mussels with a prevalence of between 20% and 90% in Shetland, Scotland (Broughton, 2016), and between 3% and 25% in South West England (Bignell et al., 2011). Thus the prevalence seen in the present study (30%) was in accordance with previous studies for U.K..

In a study undertaken on the Slovenian side of the Adriatic Sea, Gombac *et al.* (2008) described a mild infection intensity in 94% of positive mussels and moderate in 6%. In the current study, 13% (2/15) of the positive samples had a severe infection with an extremely severe infection in one sample. To the best of our knowledge, a similar intensity of infection has not been previously reported in mussels, but it could be compared with the intensity described by Spiers *et al.* (2008) in silverlip pearl oysters, where three samples out of 10,000 showed 59, 62 and 65 MPX-like ciliates in a field at 40× magnification. Nonetheless, this was only observed in a single individual mussel.

As previously reported (Gombac et al., 2008; Villalba et al., 1997; Robledo et al., 1994; Figueras et al., 1991), no signs of haemocytic response were seen in positive samples and a

disruption of some cells of the digestive gland was visible only in the severely infected sample. The lipofuscin accumulation observed in infected digestive cells could be a sign of degeneration of the cells due to the MPX presence. In molluscs, the presence of this degeneration in digestive cells has been correlated to exposure to pollution but it has also been reported as pathogen-related (Carella et al., 2015). In the heavily infected sample, the localisation of the ciliate in connective and ovarian tissue and the necrosis of these tissues without signs of evident haemocytic response were also observed. In bivalves, some parasites are able to evade the haemocytic response, being intracellular, such as *Bonamia* spp. (Carella et al., 2015). For other intracellular protozoa such as *Microcytos mackini* Farley, Volf *et* Elston, 1988, the haemocytic response is due predominantly to the necrosis of the tissue (Carella et al., 2015). *Marteilia refringens* Grizel, Comps, Bonami, Cousserans, Duthoit *et* Le Pennec, 1974 reaches the epithelial digestive cells through the epithelia of the stomach and intestine but the host response only appears after the disruption of digestive epithelium. The lack of haemocyte infiltration surrounding MPX infected digestive tubules could be correlated with the absence of a massive disruption of this epithelium. The observation of MPX in the lumen of the stomach could support the hypothesis that these ciliates enter through the alimentary canal after its ingestion (Spiers, 2008). However, this localisation was observed only in the extremely infected sample and thus might alternatively be a result of parasite exit and a route to infect other digestive tubules. On the other hand, the reported observation of the localisation of the MPX in other tissue than digestive gland does not exclude a route of entry similar to that of *M. refringens,* reaching the digestive gland after crossing the stomach and intestinal wall.

To amplify the DNA of the MPX, a fixative that allows both an easy histological identification and the count of this ciliate per slide, in addition to the amplification of DNA following laser capture microdissection, is required. In this study, 10% buffered formalin

was the best fixative for histological examination but the amplification of DNA failed in these samples. The MthC solution is known both to preserve the tissue morphology, similarly to formalin, and to maintain the integrity of DNA (Buesa, 2008). Due to the dual purpose of the present work (*i.e.* exploring an easy way to identify MPX in the tissue, and amplifying its DNA), MthC was found to be the best fixative of those tested.

Ciliates are characterised by having two types of nucleus, a germinative micronucleus and a somatic macronucleus, and two methods of reproduction, *i.e.* binary fission and conjugation (Morgens et al., 2013; Lynn, 2008). In previous studies, the observation of macronuclear division in MPX has not been reported. However, in the present study, several macronuclei were found to be dividing in the severely infected sample when observed in histological sections by light and laser scanning confocal microscopy. The division appeared as a binary fission, as reported in other Rhynchodida (Bower and Meyer, 1993). The number of nuclei observed in the present work at histological examination (up to 14) was in accordance with Robledo *et al.* (1994) who reported from 1 to 13 nuclei. From the laser scanning confocal examination after DAPI staining, the small nuclei observed at histological examination in the MPX were observed as spherical separated nuclei, varying in dimension and numbering up to 18. In the observed fission division stage, the presence of only one micronucleus was observed, thus the other small nuclei could be macronuclei, and a nuclear arrangement similar to *Urostyla grandis* Ehrenberg, 1830 could characterise MPX. In *U. grandis* multiple macronuclei fuse into a big macronucleus within a few minutes before the division (Prescott, 1994). In a previous MPX electron microscopy observation, the nucleus of MPX was supposed to be multilobed and an electrodense organelle was observed in the middle of the lobes of the nucleus and it was supposed to be the nucleolus of the multilobed nucleus (Spiers, 2008). In the present work, DAPI staining evidenced that nucleus of MPX is not multilobed and

the round corpuscle at the centre of the small nuclei was not nuclear material. It could be the contractile vacuole.

The current study has allowed description of MPX as a free-swimming ciliate in a wet-mount preparation for the first time. The typical nuclear pattern was recognizable also in the free swimming MPX. To our knowledge, this is the first description of this ciliate as a free organism, and not only intracellularly located. MPX has been previously described as Rhynchodida-like (Gombac et al., 2008) and the fresh observation of this ciliate in the present work agrees with an assignment of the membership of MPX to this order. The presence of somatic kineties which cover the entire body, and the lack of a posterior adhesive region, are typical of the order Rhynchodida (see Lynn, 2008). Only two families are present under this order, *i.e.* Sphenophryidae Chatton *et* Lwoff, 1921 and Ancistrocomidae Chatton *et* Lwoff, 1939. The first one has an intracellular adult trophic stage of various shapes (Lynn, 2008, Raabe, 1970). This stage preserves the kineties but it is unciliated while in the tomite stage the cilia are acquired on kineties (Raabe, 1970). The Ancistrocomidae are characterised by a pear or banana-shape body, a pointed anterior end, and an apical sucker (Lynn, 2008, Raabe, 1970). Both are parasites of Mollusca but Ancistrocomidae are free-swimming or attached to the host, and are not intracellular (Lynn, 2008, Raabe, 1970). In terms of intracellular behaviour, MPX is more similar to the Shenophryidae, however, morphologically it is very similar to Ancistrocomidae. Furthermore, the presence of multiple macronuclei, that characterises MPX, has not been reported in Shenophridae or Ancistrocomidae, suggesting that MPX belongs to a distinct family.

Due to the small dimensions of MPX, laser capture microdissection from unstained tissue was not possible, since the cells were rarely visible. For this reason, H&E and ethidium

bromide were tested. Both staining methods allowed identification of MPX in 3 µm sections, with best results obtained using ethidium bromide.

Most investigations of Ciliophora phylogeny are based on SSU rDNA, however, more recently a revised classification of this phylum has been published using three additional gene regions: ITS1-5,8S-ITS2 rDNA, LSU rDNA and α-tubulin (Gao et al., 2016). In the present work, the three genes SSU rDNA, LSU rDNA and α-tubulin were also employed. Despite failure of the α-tubulin gene amplification for MPX, the amplification of SSU rDNA and LSU rDNA resulted in sequences with most similarity to an uncultured phyllopharyngid sequence (85.69%) (Sauvadet et al., 2010), and to an uncultured ciliate sequence (86.45%) (Laffy, 2011). The first sequence corresponds to a phyllopharingeal ciliate sequence obtained from a genetic library of samples collected from the pallial cavity fluid of deep water mussels *Bathymodiolus thermophilus* Kenk *et* Wilson, 1985 (see Sauvadet et al*., 20*10), while the second sequence corresponds to a ciliate found in the hypobranchial gland of the sea snail *Dicathais* orbita (Gmelin, 1791) (see Laffy, 2011).

The phylogenetic analysis of both of these genes, showed that the MPX sequences clustered with H. acetinarum. Despite two orders (Hypocomatida and Rhynchodia), three families (Hypocomidae, Ancistrocomidae and Sphenophiryidae) and, overall, 29 genera and one incerta sedis (Lynn, 2008), H. acetinarum, accepted name Enigmocoma acetinarum, Hypocomatida, Hypocomidae, is the only member of the subclass Rhynchodia with a deposited sequence in GenBank. Most genera of this subclass are parasites of invertebrates, and particularly of bivalves (Lynn, 2008), however, there is a lack of molecular analyses of the members of Rhynchodia. The phylogenetic analysis performed in the current study, therefore, was not able to identify the order and the family of MPX. The moderate support of LSU (89%) and SSU (64%) MPX sequences with H. acetinarum confirmed the membership of MPX within the subclass Rhynchodia but does not support

inclusion in the order Hypocomatida, hwoever, no sequence of members of the Rhynchodida order (Ancistrocomidae and Sphenophiryidae families) have been deposed in GeneBank database for direct comparison. In the case of SSU gene, the lower support could be due to the greater number of Phyllopharyngea sequences deposited in GenBank compared to LSU Phyllopharyngea sequences, and consequentially to a more accurate analysis. The use of a short segment of SSU (653 bp) and LSU (450 bp) genes for phylogenetic analysis might have generated some artefactual structures in the phylogenetic tree, such as the clustering of the two chonotrichian species within the Cyrtophoria subclass in the SSU phylogenetic tree (Fig. 14). However, the phylogenetic analyses of both genes (SSU and LSU) confirmed the same close relationship of MPX with *H. acetinarum*, excluding a misplacing of MPX.

A previous tentative molecular characterisation of the ciliate of silverlip pearl oysters was conducted by Spiers (2008), but molecular investigation failed to amplify the DNA of the ciliate from formalin fixed samples. On the contrary, the protocol applied in the present study successfully characterised the MPX organisms.

The PCR using the primers designed on the SSU sequence confirmed the amplification of MPX DNA. In addition, this MPX amplification confirmed all histologically positive samples although it also gave positives for five out of 15 histologically negative samples. In the study of Spiers *et al.* (2008) of an MPX-like parasite from silverlip pearl oysters, the histological examination showed a sensitivity of 38.86%. The MPX PCR products reported in the present study could represent a more sensitive detection method to detect MPX than traditional histology, however, the specificity of this PCR method should be tested on several ciliates of bivalves to exclude their accidental detection. The investigation of MPX in oyster samples and more generally in other bivalve species could be important in gaining an understanding of the host and tissue preferences of this ciliate

19

and potentially its portals of entry and detailed life cycle. In addition, the use of PCR protocols described in the current study could confirm or exclude a correlation between MPX and the silverlip pearl oyster ciliate.

In the present work, several approaches to MPX characterisation were employed and assessed. Although the significance of MPX to the mussel aquaculture industry has been assumed to be negligible, a number of protocols have been developed in this study that may prove useful for the investigation of MPX and similar organisms in bivalves more widely, and may help in assessment of biology and impact. For the first time, a severe MPX infection in *Mytilus* spp. has been reported, which also showed tissue localisation in areas outside the digestive gland. The presence of tissue necrosis in this specimen appears to suggest the possibility of a pathogenic action of MPX when this ciliate localises in tissues different from the digestive gland epithelium. However, following Koch's postulates, this hypothesis cannot be confirmed without an experimental infection, and for this reason further studies should be conducted. While some aspects of the nuclear morphology and reproduction by binary fission of MPX were elucidated in the present study, detailed knowledge of the MPX life cycle nevertheless remains to be obtained.

In the present work, several free-swimming MPX ciliates were observed, and the description of the living ciliates was reported. In order to taxonomically identify this ciliate, a complete description should be performed following a silver stain impregnation (*e.g.* Klein's method). Ideally, to obtain a sufficient number of ciliates to perform this staining, a culture remains essential but the predominant intracellular localisation of the MPX makes its cultivation challenging. While phylogenetic analysis seems to confirm that MPX belongs to the order Rhynchodida it has also highlighted the current lack of molecular data on other members of the subclass Rhynchodia.

6. Acknowledgments

7. References

Bignell, J.P., Dodge, M.J., Feist, S.W., Lyons, B., Martin, P.D., Taylor, N.G.H., Stone, D., Travalent, L. & Stentiford, G.D. (2008). Mussel histopathology: Effects of season, disease and species. Aquat. Biol. 2, 1–15

Broughton, C.C. (2016). Health survey on Scottish mussels, *Mytilus edulis*, and biochemical composition analysis comparing farmed *vs* wild individuals. M.Sc. thesis, University of Stirling, UK, 38 pp.

Bower, S.M. (1992) Diseases and parasites in mussels. In: E. Gosling (ed.) The Mussel *Mytilus*: Ecology, Physiology, Genetics and culture. Elsevier Press, Amsterdam, p. 543-563.

Bower, S.M. & Meyer, G.R. (1993). *Stegotricha enterikos* gen.nov., sp.nov. (class Phyllopharyngea, order Rhynchodida), a parasitic ciliate in the digestive gland of Pacific oysters (*Crassostrea gigas*), and its distribution in British Columbia. Can. J. Zool. 71, 2005–2017

Bower, S.M. (2013). Synopsis of Infectious Diseases and Parasites of Commercially Exploited Shellfish: Intracellular Ciliates of Mussels. Available from: http://www.dfompo.gc.ca/science/aahsaa/diseasesmaladies/icmueng.html [Accessed April 2017]

Buesa, R.J. (2008). Histology without formalin? Ann. Diagn. Pathol. 12, 387–396

Carella, F. & De Vico, G., (2012). Patogeni, simbionti e lesioni correlate in *Mytilus galloprovincialis*: uno studio sullo stato di salute delle acque campane. Proceedings

of the 1st National Congress of Società Italiana di Ricerca Applicata alla Molluschicoltura, 29-30.

Carella, F., Feist, S.W. Bignell, J.P. De Vico, G. (2015). Comparative pathology in bivalves: Aetiological agents and disease processes. J. Vet. Parasitol. 131, 107–120

Cova, A.W., Serafim Júnior, M., Boehs, G. & De Souza, J.M. (2015). Parasites in the mangrove oyster *Crassostrea rhizophorae* cultivated in the estuary of the Graciosa River in Taperoá, Bahia. Brazilian. J. Vet. Parasitol. 24, 21–27

Elston, R.A., Cheney, D., Frelier, P. & Lynn, D. (1999). Invasive orchitophryid ciliate infections in juvenile Pacific and Kumomoto oysters, *Crassostrea gigas* and *Crassostrea sikamea*. *Aquaculture* 174, 1–14

Figueras, A.J., Jardon, C.F. & Caldas, J.R. (1991). Diseases and parasites of rafted mussels (*Mytilus galloprovincialis* Lmk): preliminary results. *Aquaculture* 99, 17–33.

Gao, F., Warren, A., Zhang, Q., Gong, J., Miao, M. & Sun, P. (2016). The all-data-based evolutionary hypothesis of ciliated protists with a revised classification of the phylum Ciliophora (Eukaryota , Alveolata). Sci. Rep. 6:24874

Gombac M., Pogacnik, M., Fonda, I. & Jencic, V. (2008). Intracellular ciliates of cultured mediterranean mussel (*Mytilus galloprovincialis*) in the Gulf of Trieste in Slovene Adriatic Sea. Bull. Eur. Assoc. Fish Pathol. 28, 217–221

Gouy, M., Guindon, S. & Gascuel, O. (2010). SeaView version 4: a multiplatform graphical user interface for sequence alignment and phylogenetic tree building. Mol. Biol. Evol. 27, 221−224

Hall, T.A. (1999). BioEdit: a user-friendly biological sequence alignment editor and analysis program for Windows 95/98/NT. Nucl. Acids. Symp. Ser. 41, 95-98

Laffy, P. (2011). Evolution, gene expression and enzymatic production of Tyrian purple: A molecular study of the Australian muricid *Dicathais orbita* (Neogastropoda: Muricidae). PhD thesis, Flinders University, Australia, 82-108

Lynn, D.H. (2008). The ciliated protozoa: characterization, classification and guide to the literature. 3rd edition, Springer Verlag, 605 pp.

McGurk, E.S., Ford, S. & Bushek, D. (2016). Unusually abundant and large ciliate xenomas in oysters, *Crassostrea virginica*, from Great Bay, New Hampshire, USA. J. Invertebr. Pathol. 137, 23–32

Morgens, D.W., Lindbergh, K.M., Adachi, M., Radunskaya, A. & Cavalcanti, A.R.O. (2013). A model for the evolution of extremely fragmented macronuclei in ciliates. *PLoS One* 8 (5), e64997

Prescott, D.M. (1994). The DNA of Ciliated Protozoa. Microbiol. Rev. 58, 233–267

Puchtler, I., Waldrop, F.S., Meloan, S.N. & Terry, M.S. (1970) Methacarn (Methanol-Carnoy) fixation. Practical and theoretical considerations. Histochemie 21, 97–116

Raabe, Z. (1970). Ordo Thigmotricha (Ciliata—Holotricha) III Familiae Ancistrocomidae et Sphenophryidae. Acta Protozool. 8 (31-37), 384-536

Robledo, J.A.F., Santarém, M.M. & Figueras, A. (1994). Parasite loads of rafted blue mussels (*Mytilus galloprovincialis*) in Spain with special reference to the copepod, *Mytilicola intestinalis*. Aquaculture 127, 287–302

Robledo, J.A.F., Vasta, G.R. & Record, N.R. (2014). Protozoan parasites of bivalve molluscs: Literature follows culture. PLoS One 9 (6): e100872.

Sauvadet, A., Gobet, A. & Guillou, L. (2010). Comparative analysis between protist communities from the deep-sea pelagic ecosystem and specific deep hydrothermal habitats. Environ. Microbiol. 12 (11), 2946-2964

Spiers, Z.B. (2008). The identification and distribution of an intracellular ciliate in pearl oysters, Pinctada maxima (Jameson 1901). PhD thesis, Murdoch University, Australia, 254 pp.

Spiers, Z.B., Bearham, D., Jones, J.B., O'Hara, A.J. & Raidal, S.R., (2008). Intracellular ciliated protozoal infection in silverlip pearl oysters, *Pinctada maxima* (Jameson, 1901). J. Invertebr. Pathol. 99, 247–253

Villalba, A., Mourelle, S.G., Carballal, M.J. & López, C. (1997). Symbionts and diseases of farmed mussels *Mytilus galloprovincialis* throughout the culture process in the Rias of Galicia (NW Spain). Dis. Aquat. Organ. 31, 127–139

Xu, K., Song, W. & Warren, A. (2000). Observations on trichodinid ectoparasites (Ciliophora: Peritricha) from the gills of maricultured molluscs in China, with descriptions of three new species of *Trichodina* Ehrenberg, 1838. Syst. Parasitol. 45, 17–24

Zeidan, G.C., Luz, M.D.S.A. & Boehs, G. (2012). Parasites of economically important bivalves from the southern coast of Bahia State, Brazil. Rev. Bras. Parasitol. Vet. 21, 391–398.

Figure 1: Sample of *Mytilus edulis* with more than 10^3 ciliates per slide (10% buffered formalin fixation and H&E staining): a) Severely infected digestive tubules with disruption of epithelial cells, lipofuscin granules (small arrows) and free ciliates in the lumen (big arrows); b) MPX (big arrows) and some haemocytes (small arrows) in necrotic tissue around the infected digestive tubules; c) Free MPX (arrows) in the lumen of the stomach; d) MPX (arrows) in necrotic ovarian tissue.

Figure 2: Two MPX within the same epithelial cell (big arrow) of *Mytilus edulis* and two MPXs with multi-lobed nuclei (small arrows), H&E

Figure 3: Several stages of MPX in epithelial cells of digestive tubules of *Mytilus edulis* a) MPX with a big macronucleus and a visible cytopharynx (arrow); b) MPX with macronucleus in division and two micronuclei (arrows); c) MPX with globular macronucleus and micronucleus (arrow); d) MPX with several small nuclei with different sizes and a less stained circular organelle surrounded by small nuclei (arrow). H&E

Figure 4: DAPI staining of MPX nuclei in digestive epithelial cells of *Mytilus edulis* after fixing in formalin and staining with eosin viewed using laser scanning confocal microscopy: a) large macronucleus (arrow) with several smaller nuclei; b) macronucleus in division (arrow); c) very small DAPI stained organelles in both poles of the macronucleus; d) non-DAPI stained round organelle (arrows) surrounded by small nuclei; e) same pictures with only DAPI stained nuclei; d) non-DAPI stained round organelle (arrows) surrounded by small nuclei.

Figure 5: a) Wet preparation of live free-swimming MPX following compression of the digestive gland of *Mytilus edulis*; b) Ethidium bromide (0.001%) staining of the MPX (arrows) in 3 µm slice of the digestive gland of *Mytilus edulis* for laser capture microdissection using triple fluorescence filter (MthC solution fixed).

Figure 6: Phylogenetic analysis of MPX LSU gene sequence with the sequences of Phyllopharyngea species deposited in GenBank and, when possible, the sequences of the species that showed the highest similarity with the obtained sequencing product in nucleotide BLAST for each family of Ciliophora reported by Gao *et al.* (2016). Phylogenetic trees were generated on the basis of maximum-likelihood probability with a PhyML mode using SEAVIEW and the confidence levels were calculated using bootstrapping (1000 replicates). Bootstrap values under 50% are omitted.

Figure 7: Phylogenetic analysis of MPX SSU gene sequence with the sequences of Phyllopharyngea species deposited in GenBank and, when possible, the sequences of the species that showed the highest similarity with the obtained sequencing product in nucleotide BLAST for each family of Ciliophora reported by Gao *et al.* (2016). Phylogenetic trees were generated on the basis of maximum-likelihood probability with a PhyML mode using SEAVIEW and the confidence levels were calculated using bootstrapping (1000 replicates). Bootstrap values under 50% are omitted.
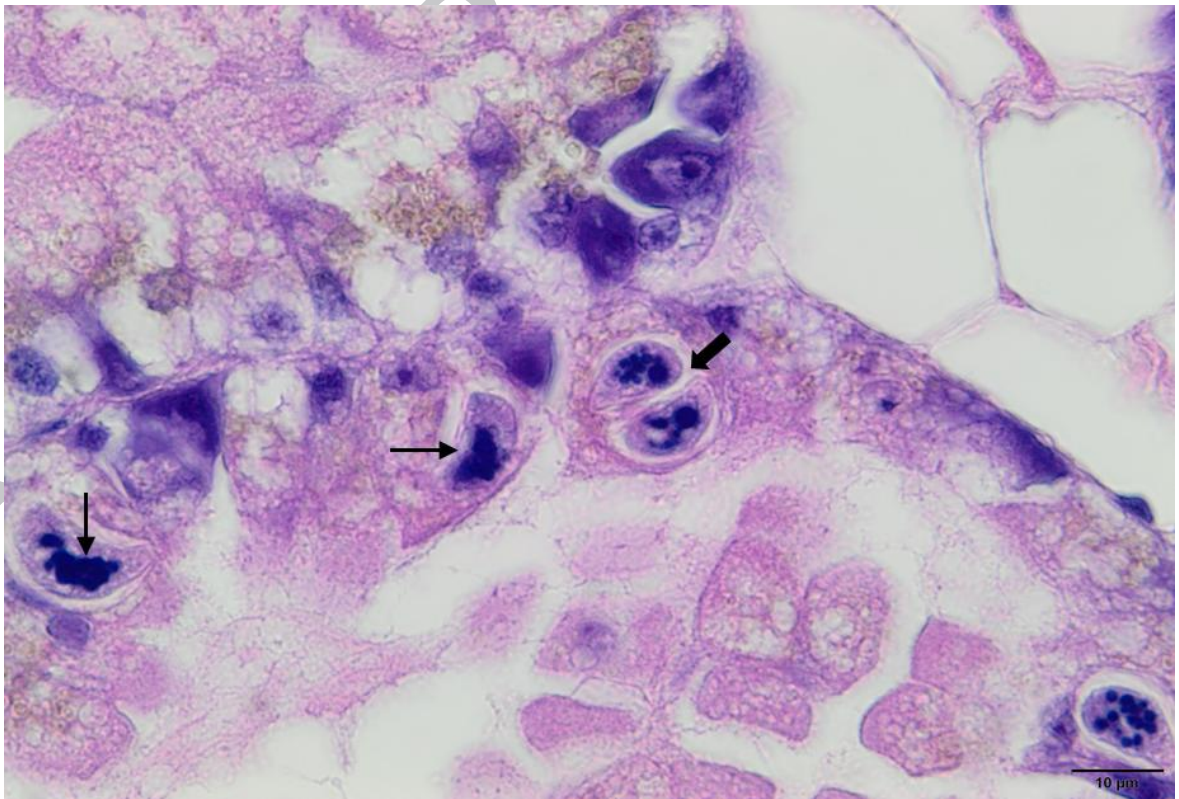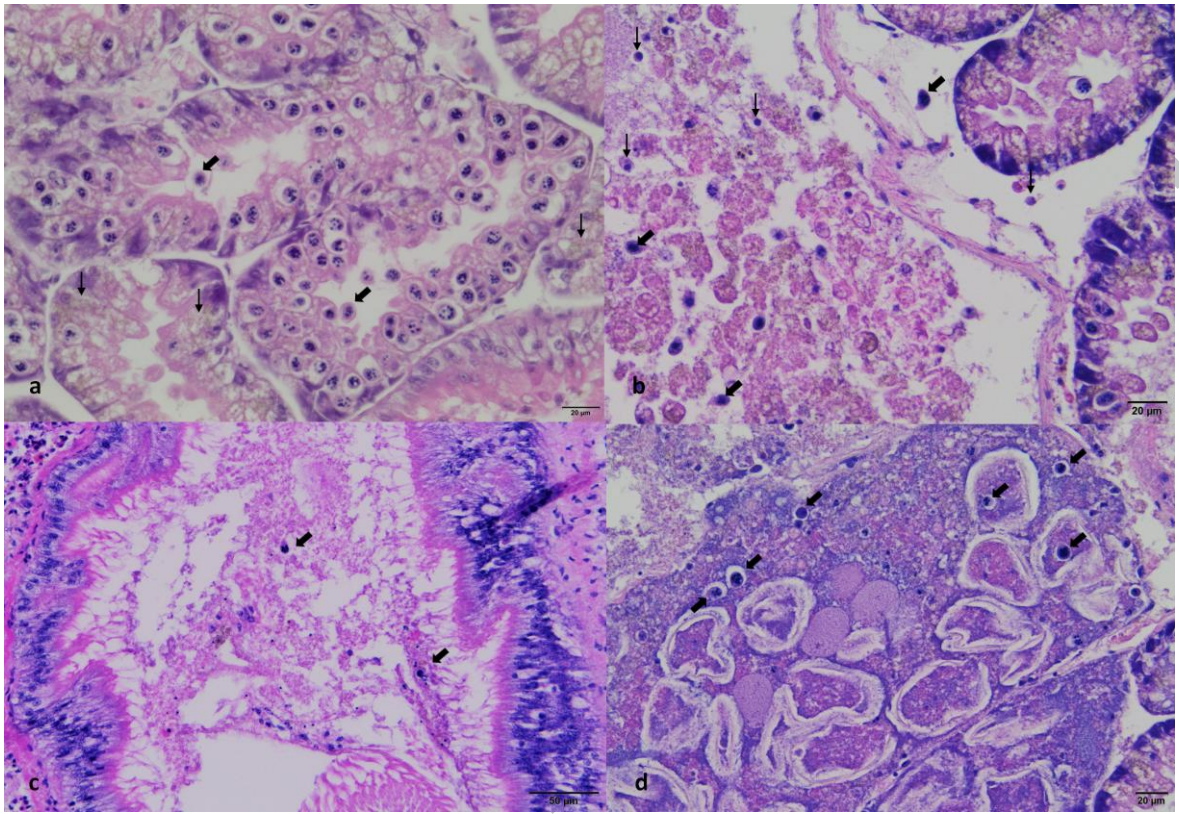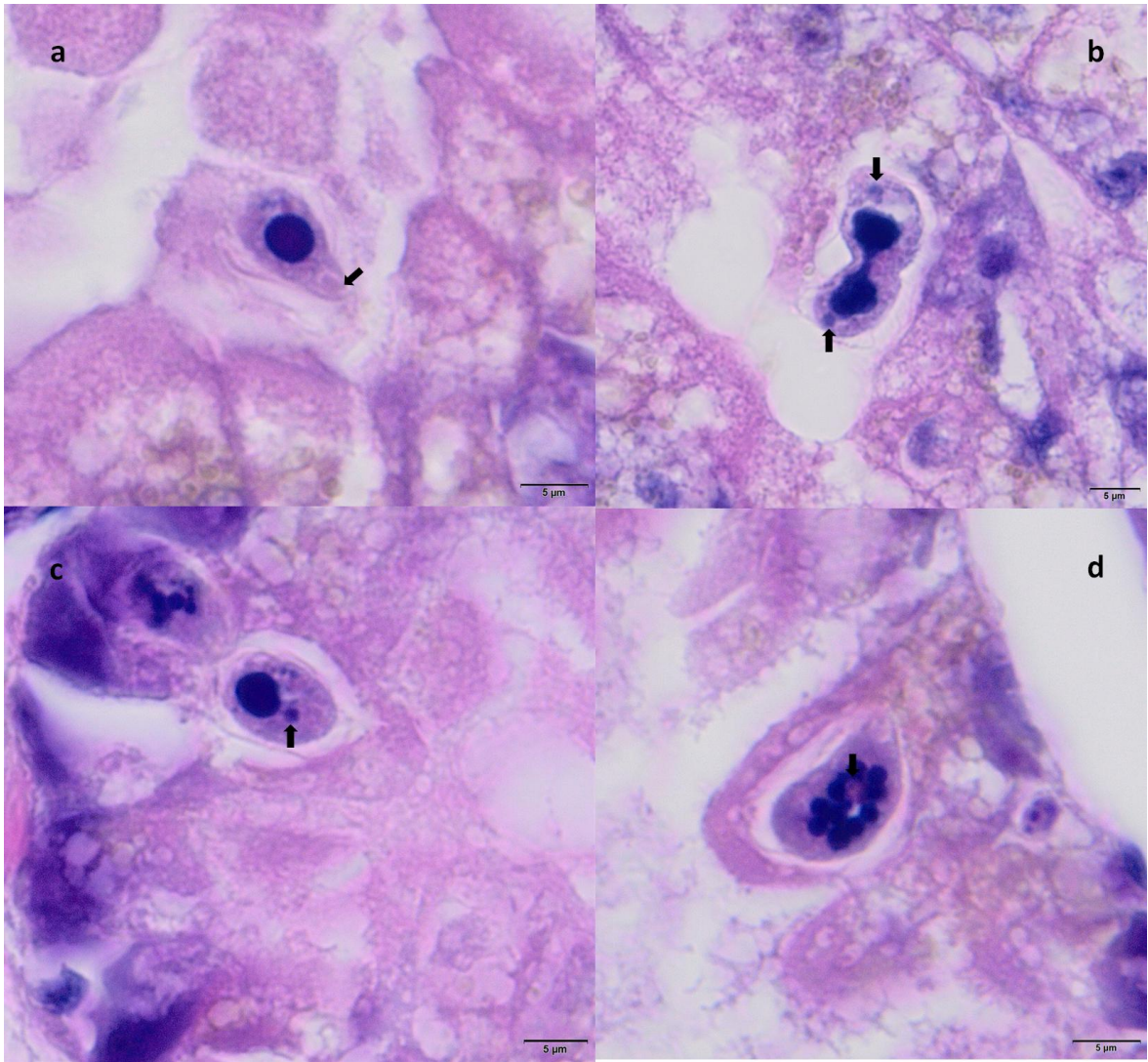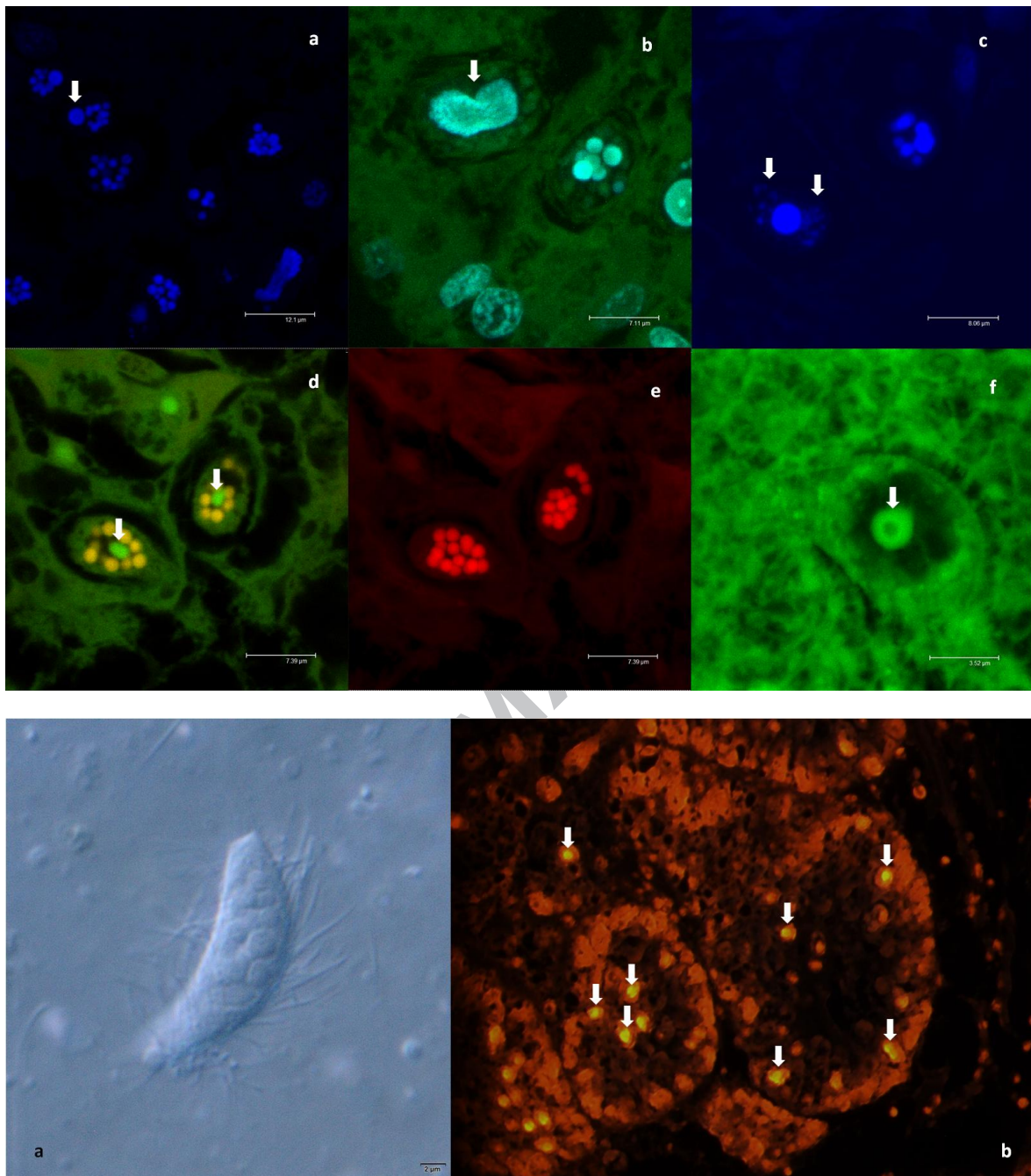
Mussel Protozoan X (class Phyllopharyngea, subclass Rhyncodia ,order Rhynchodida) in *Mytilus edulis*: fresh, histological and laser scanning confocal examination

Legend:
- ■ Rhynchodia
- ■ Suctoria
- ■ Cyrtophoria

Scale: 0.05

Tree tips:
- *Placus salinus* KC832959
- *Vorticella* sp. KM222177 — 69
- *Zoothamnium hentscheli* KM222178
- *Opisthonecta* sp. KM222179 — 59
- *Epistylis* sp. KM222174 — 100
- *Lembadion* sp. KM222173 — 63
- *Cardiostomatella vermiformis* JX310024
- *Plagiopogon loricatus* KC771339 — 78
- *Prorodon ovum* KC771340
- *Paranassula* sp. KC832964
- *Protocyclidium citrullus* KF256824 — 62
- *Ancistrum crassum* KF256825 — 89
- *Boveria subcylindrica* KF256826 — 77
- *Hippocomos salinus* JX310023
- *Philasterides armatalis* JN885120 — 91
- *Uronema* sp. JN885126 — 97
- *Pseudocohnilembus hargisi* JN885122
- *Frontonia sinica* KJ475279 — 87
- *Paramecium tetraurelia* AF149979
- *Tetrahymena pyriformis* X54004
- *Parafurgasonia* sp. KM222159 — 79
- *Nassula labiata* KC832957
- *Hypocoma acinetarum* KM222157 — 89
- **MPX** — 61
- *Ephelota gemmipara* KM222158
- *Trithigmostoma cucullulus* KM222156 — 98
- *Dysteria derouxi* KC832960
- Phyllopharyngea
- *Anigsteinia clarissima* KM222166 — 100
- *Peritromus faurei* KM222169 — 58
- *Condylostoma magnum* KM222163
- *Folliculina simplex* KM222168 — 100
- *Climacostomum virens* KM222165
- *Discocephalus rotatorius* KM222138 — 58
- *Caryotricha minuta* KM222125
- *Amphileptus marinus* JF975389 — 100
- *Phialina salinarum* JF975395
- *Apokeronopsis bergeri* JQ424840
- *Hemigastrostyla enigmatica* KM222124
- *Strongylidium orientale* KM222122
- *Pseudokahliella marina* KM222133 — 44
- *Spirotontonia turbinata* KU525739
- *Oxytricha granulifera* AF508762 — 82
- *Halteria grandinella* AF508759
- *Trachelostyla pediculiformis* KM222127 — 86
- *Strombidinopsis batos* KM222148 — 56
- *Rhizodomus tagatzi* KU715783 — 84
- *Pelagostrobilidium minutum* KM222149
- *Certesia quadrinucleata* KM222143
- *Gastrocirrhus monilifer* KM222142
- *Diophrys appendiculata* JF694057
- 74

Legend:
- Suctoria
- Rhynchodia
- Cyrtophoria
- Chonotrichia

100 Acineta compressa FJ865205
Acineta tuberosa FJ865206
Paracineta limbata FJ865207
95 Acineta flava HM140400
98 Ephelota truncata EU600182
Ephelota gigantea AB979870
Ephelota plana AB979871
100 Ephelota mammillata EU600181
76 84 Ephelota gemmipara EU600180
Heliophrya erhardi AY007445
57 MPX
64 Hypocoma acinetarum JN867019
Aporthotrochilia pulex HQ605947
88 100 Cosloperix sleighi KC753489
90 Cosloperix sp. FJ998034
96 Lynchella minuta KX364494
Lynchella nordica FJ868203
51 Chlamydonellopsis calkinsi KC753487
67 Chlamydonellopsis calkinsi FJ998033
98 100 Chlamydonella pseudochilodon FJ998032
95 Chlamydonella derouxi KJ509198
Chlamydonella irregularis KC753486
Pithites vorax FJ870070
98 99 Dysteria lanceolata KC753490
Dysteria semilunaris KX258194
100 Dysteria crassipes KC753493
61 Dysteria cristata KC753488
55 Microdysteria decora JN867020
Dysteria derouxi KX302697
75 Dysteria proraefrons KM103261
81 Dysteria nabia KM103262
96 59 Dysteria paraprocera KM103263
66 Dysteria procera DQ057347
Spirodysteria kahli KC753499
75 Dysteria pectinata FJ870068
Trochilia petrani JN867016
86 Agnathodysteria littoralis KC753482
Brooklynella sinensis KC753483
98 Trochilioides recta JN867017
96 Heterohartmannula fangi HQ605946
100 Isochona sp. AY242119
94 Chilodochona carcini KU588417
Chlamydodon triquetrus AY331795
72 Chlamydodon caudatus JQ904058
Chlamydodon excocellatus AY331793
Chlamydodon salinus JQ904057
Chlamydodon paramnemosyne JQ904059
100 Paracyrtophoron tropicum FJ998035
100 Chlamydodon obliquus FJ998030
Platyophrya spumacola KJ873051
Plagiocampa sp. KC832950
66 Placus striatus HM051057
Pinacocoleps tesselatus KC349950
Prorodon viridis U97111
Kalometopia duplicata KJ873050
87 Epistylis wuhanensis KU869709
100 Zoothamnium pelagicum DQ868351
99 Vorticella astyliformis GQ872427
70 Telotrochidium cylindricum KU363247
Tetrahymena australis KT334373
Urocentrum sp. LN870148
Entorhipidium tenue AY541688
75 Thyrophylax vorax AY541686
59 Entorhipidium triangularis AY541690
84 Uronema nigricans JF973324
99 Glauconema trihymene GQ214552
79 Pseudocohnilembus marinus Z22880
Paramecium caudatum KX302699
95 Paranassula sp. FJ998039
89 Frontonia paramagna KJ475306
Lembadion sp. KM222113
99 Ancistrum crassum JQ956537
100 Boveria subcylindrica HQ445965
89 Cyclidium glaucoma DQ442840
Hippocomos salinus JX310012
Pseudocollinia oregonensis HQ591473
Naxella paralucida KY652918
80 Parafurgasonia sp. KC832955
Kiitricha marina AY896768
55 Trachelius ovum KJ680554
100 Hemiophrys macrostoma AY102173
Fuscheria uluruensis KF733753
64 Phialina salinarum EU242508
Licnophora lyngbycola DQ445606
Diophrys sp. HE664174
Gonostomum strenuum AJ310493
Apokeronopsis sinica FJ461474
67 Stichotricha aculeata KR701611
Deviata parabacilliformis KJ766111
Urosoma sp. KY922826
Halteria sp LN869986
Certesia quadrinucleata KM222097
70 Metacylis angulata KY290322
80 Ptychocylis minor KY290321
63 100 Pelagostrobilidium paraepacrum FJ876963
Strombidinopsis sp. JX178771
74 Spirotontonia taiwanica FJ715634
96 Gastrocirrhus monilifer DQ864734
Paradiscocephalus elongatus EU684746
100 Geleia swedmarkii AY187933
Remanella microstoma JX015373
54 Climacostomum sp. LN870010
55 Aristeria clarissima KR815914
Eufolliculina uhligi U47620
74 Condylostoma magnum KM222108
99 Peritromus kahli KP970237

Phyllopharyngea

0.05

Table 1: Primers designed on gene sequences for α-tubulin, small subunit ribosomal RNA

(SSU) and large subunit ribosomal (LSU) RNA of Phyllopharyngea

Primer	Forward (5 '-3 ')	Reverse (5 '-3 ')	Amplicon size
α-tubulin Phyll	CAACTTCGCCAGAGGTCACT	TGGTAGTTGATHCCGCACTT	~750 bp
LSU Phyll	GCTGGTTCC CTCTGAAGTTTC	CTATGCCCTCGCCCTCTTACT	~450 bp
SSU Phyll	TGGTAGTGTATTGGACTACCA	CATACTCCCCCMAGAACCCAA	~750 bp

31

- First description of fresh Mussel Protozoan X
- The nuclear pattern of MPX was elucidated by Confocal Laser Microscopy examination
- First report of not digestive gland localization of MPX was described in *M. edulis*
- Phylogenetic analyses of MPX LSU and SSU genes was performed
- Specific MPX PCR on SSU gene was performed